2009

# Estimation of chlorophyll-a concentration in case II waters using MODIS and MERIS data—successes and challenges

Wesley J. Moses
*University of Nebraska at Lincoln*, wmoses.unl@gmail.com

Anatoly A. Gitelson
*University of Nebraska at Lincoln*, agitelson2@unl.edu

V. Povazhnyy
*Southern Scientific Center of the Russian Academy of Sciences*

Environ. Res. Lett. **4** (2009) 045005 (8pp) doi:10.1088/1748-9326/4/4/045005

# Estimation of chlorophyll-*a* concentration in case II waters using MODIS and MERIS data—successes and challenges

**W J Moses[1], A A Gitelson[1], S Berdnikov[2] and V Povazhnyy[2]**

[1] Center for Advanced Land Management Information Technologies (CALMIT), School of Natural Resources, University of Nebraska-Lincoln, USA
[2] Southern Scientific Center of the Russian Academy of Sciences, Rostov-on-Don, Russia

E-mail: wmoses@calmit.unl.edu

Received 13 February 2009
Accepted for publication 9 July 2009
Published 15 October 2009
Online at stacks.iop.org/ERL/4/045005

**Abstract**

We present and discuss here the results of our work using MODIS (moderate resolution imaging spectroradiometer) and MERIS (medium resolution imaging spectrometer) satellite data to estimate the concentration of chlorophyll-*a* (chl-*a*) in reservoirs of the Dnieper River and the Sea of Azov, which are typical case II waters, i.e., turbid and productive. Our objective was to test the potential of satellite remote sensing as a tool for near-real-time monitoring of chl-*a* distribution in these water bodies. We tested the performance of a recently developed three-band model, and its special case, a two-band model, which use the reflectance at red and near-infrared wavelengths for the retrieval of chl-*a* concentration. The higher spatial resolution and the availability of a spectral band at around 708 nm with the MERIS data offered great promise for these models. We compared results from several different atmospheric correction procedures available for MODIS and MERIS data. No one particular procedure was consistently and systematically better than the rest. Nevertheless, even in the absence of a perfect atmospheric correction procedure, both the three-band and the two-band models showed promising results when compared with *in situ* chl-*a* measurements. The challenges and limitations involved in satellite remote monitoring of the chl-*a* distribution in turbid productive waters are discussed.

**Keywords:** remote sensing, MODIS, MERIS, chlorophyll-*a*, turbid productive waters

## 1. Introduction

Phytoplankton biomass is an important bio-physical characteristic that is commonly used to assess the eutrophic status of water bodies. The photosynthetic pigment chlorophyll-*a* (chl-*a*) is a key indicator of phytoplankton biomass. Thus the estimation of chl-*a* concentration is critically integral to monitoring water quality.

Photoactive pigments such as chl-*a* cause distinct changes in the color of water by absorbing and scattering the light incident on water. Chl-*a* concentration can be estimated from remotely sensed spectral reflectance data by relating optical changes observed in the reflected light at specific wavelengths to the concentration of chl-*a*. The ease of this procedure depends on the optical characteristics of the water body. In deep ocean waters, phytoplankton is usually the predominant constituent and the concentrations of other constituents co-vary with chl-*a* concentration. Thus, the optical properties of these waters are dominated by phytoplankton and the observed spectral features in the reflected light can be directly related to chl-*a* concentration. Such waters are commonly referred to as case I waters (Morel and Prieur 1977). For case I waters, spectral algorithms that use reflectances in the blue and green regions of the spectrum (blue–green ratios) have been shown to yield accurate estimates of chl-*a* concentration (Gordon and Morel 1983, Gordon *et al* 1988, O'Reilly *et al* 2000). In most inland, estuarine, and coastal waters, constituents such as suspended solids and dissolved organic matter occur in abundance and their concentrations do not co-vary with chl-*a* concentration. Thus phytoplankton does not solely

 

dominate the optical properties of such turbid productive waters, commonly referred to as case II waters (Morel and Prieur 1977). The optical complexity of case II waters, specifically, the overlapping and uncorrelated absorptions by dissolved organic matter and non-algal particles in the blue region of the spectrum, renders the blue–green ratios inaccurate for estimating chl-*a* concentration (Carder *et al* 2004, Darecki and Stramski 2004, Dall'Olmo *et al* 2005). Thus, for estimating chl-*a* concentration in turbid productive waters, spectral algorithms that are based on reflectance in the red and the near-infrared (NIR) spectral regions are preferable (Gitelson 1992, Gons 1999, Gower *et al* 1999, Dall'Olmo *et al* 2005).

Using reflectance data collected with field spectrometers, Dall'Olmo and Gitelson (2005) and Gitelson *et al* (2008) demonstrated that the NIR–Red models, given by,

The three-band NIR–Red model:

$$\text{chl-}a \propto (R_{\lambda_1}^{-1} - R_{\lambda_2}^{-1}) \times R_{\lambda_3} \quad (1)$$

and its special case,

The two-band NIR–Red model (Gitelson 1992):

$$\text{chl-}a \propto (R_{\lambda_1}^{-1}) \times R_{\lambda_3} \quad (2)$$

give accurate estimates of chl-*a* concentration for turbid and productive waters with a wide range of bio-physical and optical characteristics. It was also shown that the NIR–Red models work well when the waveband locations and widths are chosen to match the wavebands of MODIS (moderate resolution imaging spectroradiometer) and MERIS (medium resolution imaging spectrometer).

In this study, we tested the NIR–Red models (equations (1), and (2)) for estimating chl-*a* concentration using MODIS and MERIS data acquired over the Kremenchug Reservoir and the Dnieper Estuary in Ukraine and the Azov Sea in Russia, which are all turbid and productive waters and fall under the class of case II waters.

MODIS delivered daily images of the study area while MERIS, with a longer revisit cycle, yielded an image every two–three days. Nevertheless, MERIS had a significant advantage over MODIS with respect to the estimation of chl-*a* concentration due to its possession of a spectral band at 708 nm and its higher spatial resolution (260 m × 290 m compared to 1 km × 1 km for MODIS).

When applying the NIR–Red models to satellite data, the problem takes a broader dimension. On the one hand, the accuracy of the models depends on their ability to account for the variations in the bio-physical and optical characteristics of water. On the other hand, factors such as the interference of the intervening atmosphere and the very low magnitude of water reflectance in the NIR region also affect the accuracy of the models. Moreover, the temporal difference between the *in situ* and satellite data acquisitions and the difference between the spatial resolutions of the *in situ* and satellite measurements make it difficult to calibrate the models.

In this letter we report the results and the challenges in using the NIR–Red models for satellite data over turbid and productive waters.

## 2. Data and methods

The *in situ* data consisted of analytical measures of the concentrations of chl-*a* and TSS (total suspended solids) and related ancillary water quality data. These data were collected by the crews at the Southern Scientific Centre of the Russian Academy of Sciences, Rostov-on-Don, Russia and the Institute for Environmental Quality, Kiev, Ukraine. Water samples were collected at each station, filtered through Whatman GF/F glass filters and analyzed for chl-*a*, TSS and other ancillary data. Chl-*a* was measured through extraction in hot ethanol.

MODIS and MERIS data were used in this study. Satellite data acquired up to two days before or after the date of *in situ* data collection were used in cases where same-day images were not available.

Four different options were considered for atmospherically correcting the MODIS data. The difference among these procedures lies in how the aerosol contribution to the data recorded at the sensor is accounted for.

(a) *NIR bands procedure*: this is essentially the atmospheric correction procedure developed by Gordon and Wang (1994) wherein the radiance recorded at the NIR wavebands centered at 748 and 869 nm are used to select the aerosol model for the area imaged. This procedure assumes zero water-leaving radiance in the NIR wavebands.

(b) *SWIR bands procedure*: in reality, the assumption of zero water-leaving radiance in the NIR wavebands does not hold true for turbid waters (Hu *et al* 2000, Ruddick *et al* 2000, Wang and Shi 2005). In this procedure, the SWIR (short wave infrared) bands centered at 1240 and 2130 nm, where even turbid water is very dark, are used for aerosol model selection (Wang and Shi 2005).

(c) *Wang–Shi procedure*: this is the same as the '*SWIR bands procedure*' but with different calibration coefficients for the SWIR bands (Wang and Shi 2005).

(d) *MUMM correction*: this procedure was developed by the management unit of the North Sea mathematical models (MUMM). The usual assumption of zero water-leaving radiance in the NIR bands is replaced by the assumption of spatial homogeneity of the 748/869 reflectance ratio for aerosol and water reflectance within an image (Ruddick *et al* 2000). This ratio calculated for aerosol and water reflectance is used to determine the aerosol model.

Two types of atmospheric correction were considered for MERIS data.

(e) *Bright pixel atmospheric correction:* this is a modification of the standard atmospheric correction procedure routinely applied to MERIS images. (Moore *et al* 1999, Aiken and Moore 2000). This involves classifying the pixels into case I and case II water pixels based on the radiance recorded by the sensor at 708 nm. The case I pixels have zero water-leaving radiance in the NIR region. For these pixels, the at-sensor radiance recorded at 708 nm is assumed to have been entirely due to atmospheric contribution and these pixels are subjected to the conventional atmospheric correction procedure according to Gordon and Wang (1994). For the case

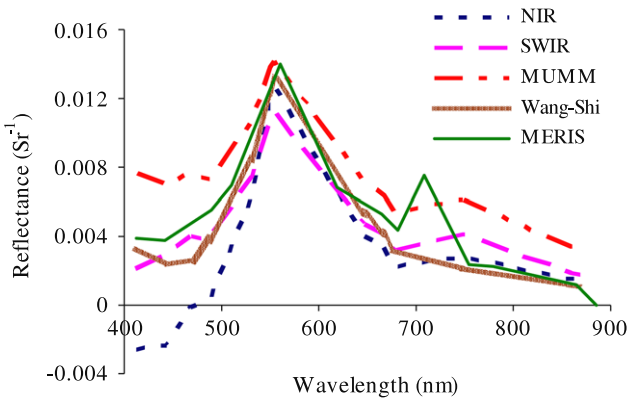


**Figure 1.** Reflectance spectra for the same station (chl-*a* 39.17 mg m$^{-3}$) retrieved using different atmospheric correction procedures.

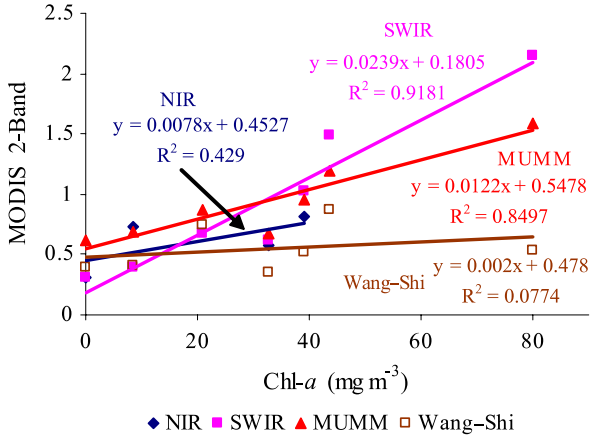


**Figure 2.** Two-band NIR–Red model (equation (3)) values versus chl-*a* concentration for different atmospheric correction procedures for MODIS data.

II pixels, the radiances recorded at the NIR wavebands are used in an iterative procedure to isolate the water-leaving radiance and thus factor out the aerosol scattering at these wavelengths. This estimated measure of aerosol scattering is then used in the same procedure as Gordon and Wang's (1994) to extrapolate the aerosol scattering at shorter wavelengths and retrieve the water-leaving radiance and subsequently the remote sensing reflectance at all wavelengths.

(f) *Case 2 regional processing:* this method is a neural network based procedure developed specifically for inland and coastal case II waters that are very turbid. (Doerffer and Schiller 2007, 2008), where even the *bright pixel atmospheric correction* procedure yields negative reflectances, especially in the blue region. It is implemented as a two-step procedure—(i) a forward neural network for the retrieval of water-leaving radiances and subsequently the remote sensing reflectances from the at-sensor radiances (atmospheric correction), and (ii) a backward neural network for the retrieval of the inherent optical properties of water and subsequently the concentrations of constituents by inverting the remote sensing reflectances. Both the forward and the backward neural networks were trained based on radiances simulated by radiative transfer solutions and built to parameterize the relationships between the top-of-atmosphere radiances and the water-leaving radiances (for the forward model) and between the remote sensing reflectances and the inherent optical properties (for the backward model). The recorded radiances at 12 wavebands (at visible and NIR wavelengths) are used in the neural network.

Unless specifically stated, the MERIS results shown in this paper are from the *bright pixel atmospheric correction* procedure.

After the retrieval of remote sensing reflectance, the two-band model was applied to MODIS data and the two-band and three-band models to MERIS data as follows,

$$\text{For MODIS}: \ \text{Chl-}a \propto (R_{667}^{-1} \times R_{748}) \tag{3}$$

$$\text{For MERIS}: \text{Chl-}a \propto (R_{665}^{-1} \times R_{708}) \tag{4}$$

$$\text{Chl-}a \propto (R_{665}^{-1} - R_{708}^{-1}) \times R_{753} \tag{5}$$

where $R_x$ is the remote sensing reflectance at the waveband centered at $x$ nm. The corresponding band numbers are 13 (667 nm) and 15 (748 nm) for MODIS, and 7 (665 nm), 9 (708 nm), and 10 (753 nm) for MERIS.

## 3. Results and discussion

### *3.1. Effects of atmospheric correction*

The wavebands in the NIR–Red models are located close enough to each other that the atmospheric effects can be assumed to be almost uniform at the wavelengths considered. Thus, in principle, the models are not very sensitive to atmospheric effects. However, the water-leaving radiance is very low in the NIR region and the NIR reflectance is a multiplicative term in the models (equations (3)–(5)). Hence the models are very sensitive to changes in the magnitude of the NIR reflectance. Thus, good atmospheric correction, resulting in accurate retrievals of NIR reflectance, is crucial to the success of the model.

In order to show the differences in surface reflectances retrieved through the different atmospheric correction procedures, we compared the reflectance spectra for the same station (figure 1). The shape and magnitude of the reflectances varied widely for the different correction procedures. Consequently, the relationship between the two-band model and chl-*a* concentration also varied widely for reflectances retrieved for the same set of stations (figure 2).

Thus it is evident that the accuracy of the NIR–Red models depends on the particular atmospheric correction procedure applied to retrieve surface reflectance.

### *3.2. Chlorophyll-a estimation*

The models (equations (3)–(5)) gave reasonably close relationships with analytically measured chl-*a* concentrations (figure 3). Among the different atmospheric correction procedures for MODIS data, in terms of the ability of the

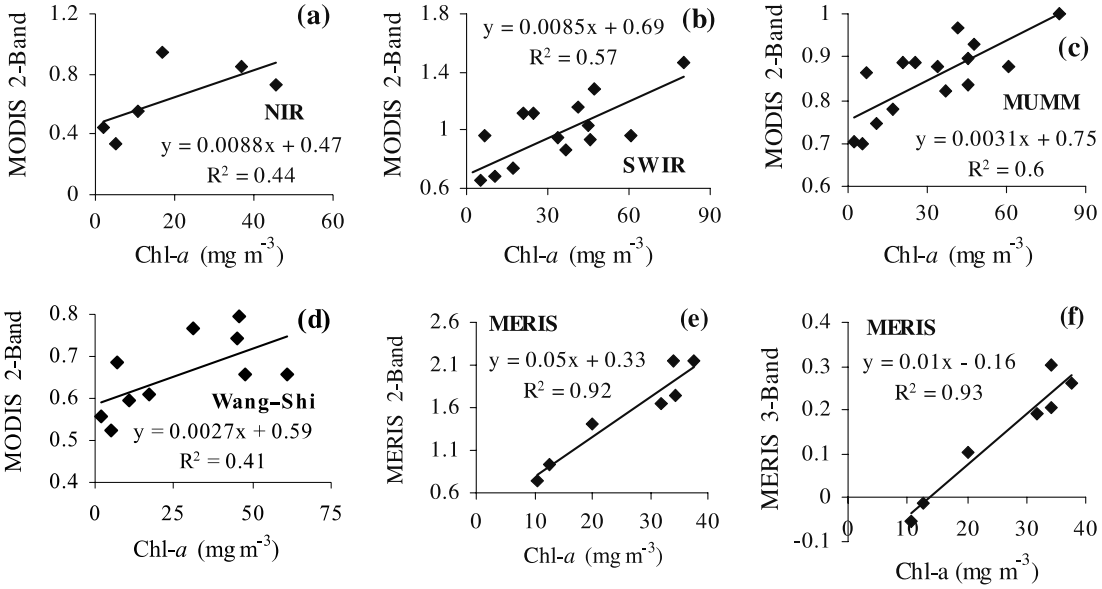


**Figure 3.** Plots of chl-*a* versus NIR–Red model values. (a)–(d): the results from MODIS data for 27 August 2003 from the Dnieper Estuary; (e) and (f): the results from MERIS data for Jun2008 from the Azov Sea.

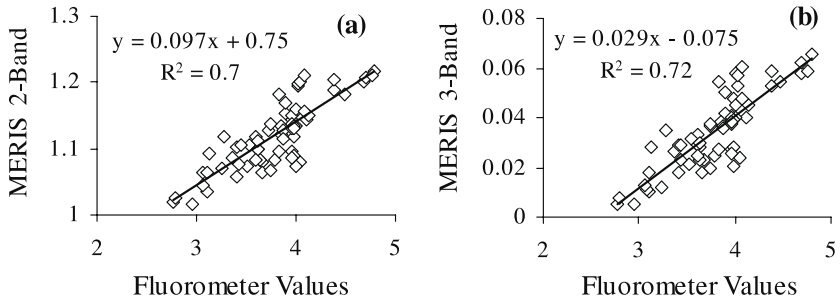


**Figure 4.** Comparison of fluorometer readings and NIR–Red model values retrieved from MERIS data: (a) two-band model, (b) three-band model.

model to explain the highest percentage of the variation in chl-*a* concentration, no one procedure stood out consistently better than the rest.

However, in general, the model values from the *SWIR bands procedure* and the *MUMM correction* compared better with chl-*a* concentration than did the model values from the other two procedures. Also, in general, the results from MERIS data were better than those from MODIS data. This is due to the availability of a spectral channel centered at 708 nm in the MERIS sensor and the higher spatial resolution of MERIS (260 m × 290 m) compared to MODIS (1 km × 1 km). The magnitude of the reflectance from water is significantly higher at 708 nm than at 748 nm. Thus the two-band model for MERIS data (equation (4)) is less sensitive to uncertainties in the retrieved NIR reflectance than is the two-band model (equation (3)) for MODIS data (Gitelson *et al* 2009). Moreover, the reflectance at 708 nm better represents the chl-induced reflectance peak in the NIR (Gitelson 1992) than does the reflectance at 748 nm. Hence the results from the two-band model for MERIS data yielded higher accuracies than the two-band model for MODIS data.

Figure 3 shows the comparisons between the NIR–Red model values and chl-*a* concentration. Figures 3(a) through (d) show the results from MODIS data for the two-band model (equation (3)). The *in situ* and satellite data were acquired on the same day (27 August 2003) from the Dnieper Estuary. The number of data points in each plot is not the same because not all station pixels were equally retrievable for the different procedures. MERIS image was not available for that date. Figures 3(e) and (f) show the results from MERIS imagery for data collected from the Azov Sea during the period 17–19 June 2008. As illustrated in the figure, in general, the model values derived from MERIS data were able to account for more than 90% of the variation in chl-*a* concentration, whereas the results from MODIS rarely accounted for more than 60%.

### *3.3. Chlorophyll fluorescence estimation*

Continuous measurements of chl-*a* fluorescence were made from a ship along a transect on the Azov Sea on 17 June 2005. Figure 4 shows comparisons between fluorometer readings and the two-band and three-band model values for MERIS data acquired on the same day. The results show that both the two-band and the three-band models are able to explain about 70% of the variation in chl-*a* fluorescence.

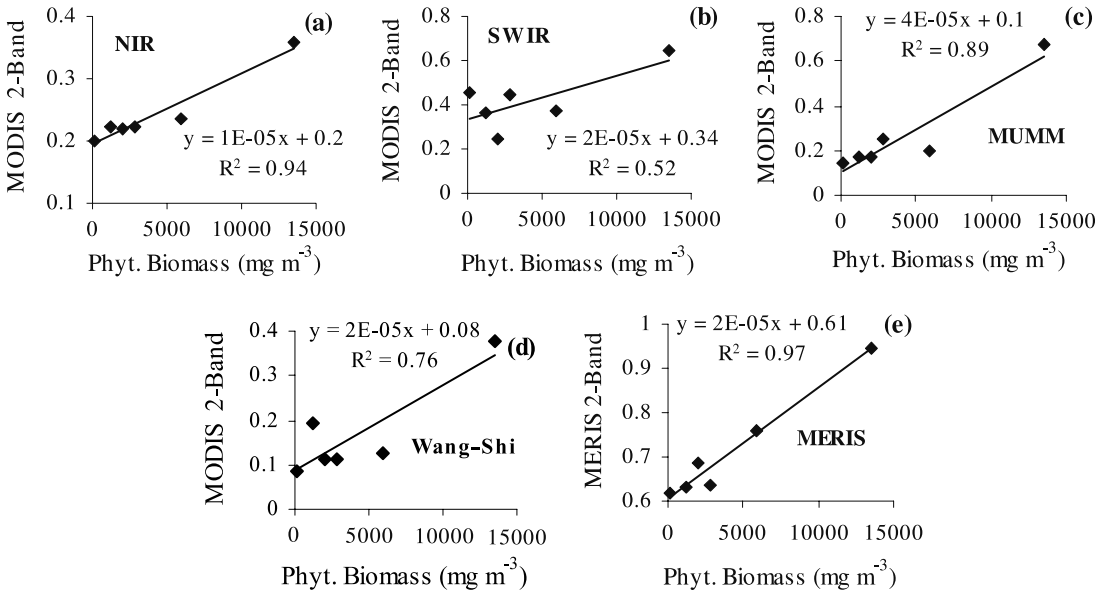


**Figure 5.** Phytoplankton biomass versus NIR–Red model values. (a)–(d): two-band model, MODIS data. (e): two-band model, MERIS data.

### *3.4. Phytoplankton biomass estimation*

Water samples were collected from the Azov Sea on 30 June and 01 July of 2006 and the phytoplankton biomass was analytically measured. Satellite images were acquired between 29 June and 01 July of 2006. Comparisons of phytoplankton biomass with the NIR–Red model values calculated for MODIS and MERIS images are shown in figure 5. The plots illustrate the ability of the models to account for about 90% of the variation in phytoplankton biomass.

### *3.5. Comparison with MERIS-estimated Chl-a values*

While analyzing the data, it was found that the three-band NIR–Red model values (equation (5)) had a consistently close relationship with the chl-*a* concentrations estimated by the default neural network based algorithm implemented in the *case 2 regional processing* procedure for MERIS images. The slope and offset of the relationship remained remarkably steady for data from multiple images from the Chesapeake Bay, the Delaware Bay and the Azov Sea (figure 6).

The Chesapeake Bay dataset contained a total of 318 data points from 10 different images; the Delaware Bay dataset contained 136 data points from 7 different images; the Azov Sea dataset contained 345 data points from 4 different images. This remarkably tight and steady relationship implies that the neural network implemented in the *case 2 regional processing* procedure converges to the three-band NIR–Red model values. Further investigation is needed to understand the reason for this close relationship.

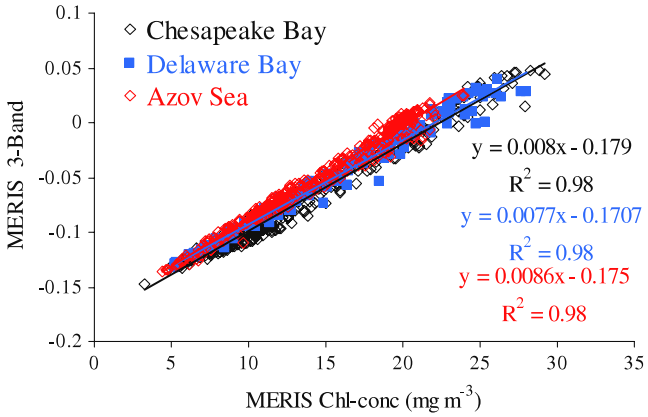


**Figure 6.** Comparison between the three-band NIR–Red model (equation (5)) and the chl-*a* concentrations predicted by the case 2 regional processing procedure for MERIS data.

## 4. Limitations and challenges

The results from proximal sensing (Dall'Olmo and Gitelson 2005, Gitelson *et al* 2008, 2009) and the results from satellite remote sensing presented here illustrate the strong correlation the NIR–Red model values have with chl-*a* concentration and hence the potential of these models to estimate chl-*a* concentration from satellite data. However, except for the results obtained from a limited dataset in one study (Moses *et al* 2009), it has not yet been possible to reliably calibrate this relationship so as to accurately estimate chl-*a* concentration in quantitative measures. The following are some of the factors that make it difficult to develop stable and reliable calibration equations.

### *4.1. Atmospheric correction*

A successful correction for atmospheric effects and an accurate retrieval of surface reflectance are crucial to the success of the NIR/Red models.

For data retrieved from satellite, the slope and offset of the linear relationship between chl-*a* and NIR–Red model values have been observed to vary across data from different dates.

However, using data from field spectrometers, Dall'Olmo and Gitelson (2005), Gitelson *et al* (2008), and Gitelson *et al* (2009) have demonstrated that the NIR–Red model values have a steady and stable relationship with chl-*a* concentration for waters with widely varying bio-physical and optical characteristics. Thus the observed differences in the slope and offset across different images ought to be attributable to issues related to the retrieval of surface reflectance from the satellite images. Unless the atmospheric correction procedure is able to uniformly correct for the often non-uniform atmospheric effects across different dates, the NIR–Red models may have substantial uncertainties when applied to multi-temporal data.

The *NIR bands procedure* is unsuitable for waters that are very turbid and have significant reflectance in the NIR region (Hu *et al* 2000, Ruddick *et al* 2000, Wang and Shi 2005) as it would result in an overestimation of the aerosol contribution and a resultant underestimation of the water-leaving radiance. Procedures that rely on SWIR bands for aerosol model selection should, in theory, work reasonably well because even turbid waters are quite dark at the SWIR region. However, the higher level of detector noise at SWIR (and the consequent lower signal–noise ratio) significantly reduces the advantage gained by using the SWIR bands for aerosol model selection. The *MUMM correction*, which was developed to prevent negative reflectances at the shorter wavelengths, often overestimated the reflectances. Figure 7 shows reflectances retrieved through the *NIR bands procedure* from the same water body for very similar values of chl-*a* concentration on three different days. The significant differences in the shape and magnitude of the retrieved reflectances (especially, the chl-*a* absorption in the red and the reflectance peak in the NIR region) mean that the NIR–Red model values will be very different for these data points with very similar chl-*a* concentrations.

Judging by the shape of the retrieved reflectance spectra, particularly the spectral features at the red and NIR wavebands caused by the presence of chl-*a* in water, the *bright pixel atmospheric correction* procedure implemented in the standard processing of MERIS data looks good. However, inconsistencies still exist and the procedure often yields negative reflectances, especially for very turbid waters. The atmospheric correction procedure implemented in the *case 2 regional processing* scheme does a better job of preventing negative reflectances. However, it was found in several instances that the chl-*a*-induced spectral features in the red and NIR wavebands were less pronounced in the output from the *case 2 regional processing* compared to the output from the *bright pixel atmospheric correction* (Moses *et al* 2009).

Without actual *in situ* measurements of water-leaving radiance taken at the time of satellite overpass, it is not possible to reliably assess the accuracy of the different atmospheric correction procedures by simply looking at the reflectance curves retrieved from the image alone.

### 4.2. Temporal variation of water quality

A satellite captures its entire swath within a matter of a few seconds whereas it takes several hours to collect *in situ* data. With the inland, estuarine, and coastal waters being quite dynamic, it is conceivable that the water might have undergone appreciable changes in its bio-physical and optical characteristics during these few hours. In our studies, differences in chl-*a* concentration of up to a factor of two have been observed within a matter of a few hours. Thus it is important that the temporal variations in the concentrations of optically active constituents such as chl-*a*, TSS, inorganic suspended matter and colored dissolved organic matter be accounted for. This problem is magnified when there is no cloud-free satellite image available for the date of *in situ* data collection and one has to use the image acquired a day or two before/after.

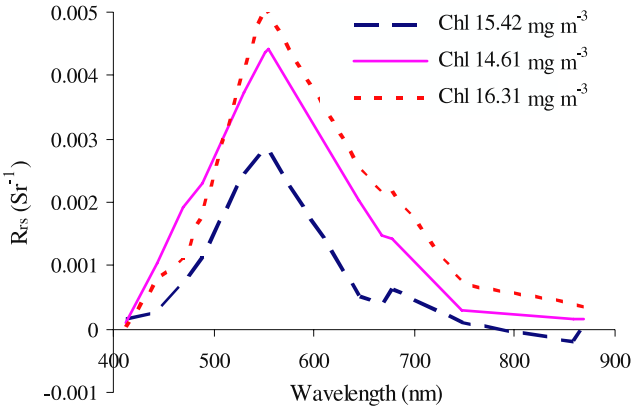


**Figure 7.** Reflectance spectra retrieved through the NIR bands procedure from MODIS data from different dates for stations with similar chl-*a* concentrations.

With the *in situ* stations spread quite far from each other, considering the satellite pixel dimension and the necessity to have stations separated by at least two pixel lengths, it has been rather difficult to collect *in situ* data using a single vessel at more than 10–12 stations within a time frame of a few hours surrounding the satellite overpass. As stated above, the bio-physical and optical characteristics at some of these stations might be different at the time of measurement from what they were at the time of satellite overpass. Furthermore, some of these stations might happen to fall under cloud cover or haze. Thus the number of stations available for comparison with same-day images is quite few, thereby making it difficult to develop reliable calibration equations for the model.

The effect of temporal variability is not uniform for all water bodies but is rather case-specific. As such, as indicated in some of our results, there have been cases where a temporal difference up to two days did not adversely effect the estimation of chl-*a* concentration due to the stable bio-physical condition of the water body. Nevertheless, it is still essential to account for the temporal variations in water quality between the time of *in situ* data collection and the time of satellite image acquisition.

### 4.3. Within-pixel spatial heterogeneity

Often, the spatial heterogeneity in the water body might be such that the point *in situ* station may not be truly representative of the satellite pixel area (260 m × 290 m for

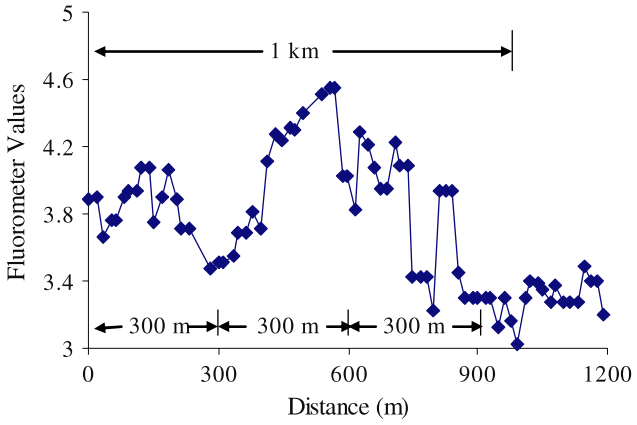


**Figure 8.** Fluorescence measurements taken continuously along a transect on the Azov Sea plotted against the distance from the starting point.

MERIS and 1 km × 1 km for MODIS) surrounding the station. In analyzing fluorescence measurements taken continuously along a transect on the Azov Sea in June 2005, significant variations were found in fluorescence values within every 300 m and 1 km lengths along the transect (figure 8). When the water within each satellite pixel is not truly homogeneous, it becomes difficult to confidently and reliably compare the satellite-derived values to point *in situ* observations.

### *4.4. Need for modified in situ data collection strategy*

The significance of the effects of the factors mentioned above and the difficulty in isolating them necessitate the development of *in situ* data collection techniques that help understand and account for these factors. In order to reliably assess the accuracy of atmospheric correction procedures, it is necessary to have actual measurements of water-leaving radiance collected *in situ* at the time of satellite overpass. Within-pixel spatial heterogeneity and temporal variation have to be accounted for by taking multiple measurements around each station so as to characterize the spatial variation within the satellite pixel area around the station and repeated measurements (at least twice, covering the length of time elapsed between the satellite overpass and the *in situ* data collection) at each station to characterize the temporal variation. If these factors are not accounted for, they present inherent hurdles to the development of reliable regression equations to calibrate the NIR–Red models. Of course, the rigor and the extent to which the *in situ* data collection procedures need to be adapted depend on the particular conditions at the water body.

## 5. Conclusion

The results have illustrated the potential of the NIR–Red models to estimate chl-*a* concentration in turbid productive waters from satellite data. However, challenges still remain in broadly applying the models to estimate absolute measures of chl-*a* concentration. With an improved atmospheric correction technique and the availability of the means and techniques to collect *in situ* datasets that account for the effects of temporal variations of the concentrations of optically active constituents and the within-pixel spatial heterogeneity of the water body, it might be possible to have a better assessment of the accuracy of the NIR–Red models.

## Acknowledgments

This research was supported by the NASA Land Use Land Cover Change Program grant NNG06GG17G to AG. Authors are thankful to the ESA Earth Observation Missions Helpdesk Team for providing MERIS data and to the University of Nebraska Agricultural Research Division, Lincoln, for providing their resources. This research was also supported in part by funds from the Hatch Act.

## References

Aiken J and Moore G 2000 *ATBD Case 2 s Bright Pixel Atmospheric Correction. PO-TN-MEL-GS-0005* (14 pp) Center for Coastal and Marine Sciences, Plymouth Marine Laboratory, UK

Carder K L, Chen F R, Cannizzaro J P, Campbell J W and Mitchell B G 2004 Performance of the MODIS semi-analytical ocean color algorithm for chlorophyll-*a Adv. Space Res.* **33** 1152–9

Dall'Olmo G and Gitelson A A 2005 Effect of bio-optical parameter variability on the remote estimation of chlorophyll-*a* concentration in turbid productive waters: experimental results *Appl. Opt.* **44** 412–22

Dall'Olmo G, Gitelson A A, Rundquist D C, Leavitt B, Barrow T and Holz J C 2005 Assessing the potential of SeaWiFS and MODIS for estimating chlorophyll concentration in turbid productive waters using red and near-infrared bands *Remote Sens. Environ.* **96** 176–87

Darecki M and Stramski D 2004 An evaluation of MODIS and SeaWiFS bio-optical algorithms in the Baltic Sea *Remote Sens. Environ.* **89** 326–50

Doerffer R and Schiller H 2007 The MERIS case 2 water algorithm *Int. J. Remote Sens.* **28** 517–35

Doerffer R and Schiller H 2008 *MERIS Regional Coastal and Lake Case 2 Water Project Atmospheric Correction ATBD. GKSS-KOF-MERIS-ATBD01* (42 pp) Institute for Coastal Research, GKSS Research Center, Geesthacht

Gitelson A 1992 The Peak near 700 nm on radiance spectra of algae and water-relationships of its magnitude and position with chlorophyll concentration *Int. J. Remote Sens.* **13** 3367–73

Gitelson A, Gurlin D, Moses W and Barrow T 2009 A bio-optical algorithm for the remote estimation of the chlorophyll-*a* concentration in case 2 waters *Environ. Res. Lett.* **4** 045003

Gitelson A A, Dall'Olmo G, Moses W, Rundquist D C, Barrow T, Fisher T R, Gurlin D and Holz J 2008 A simple semi-analytical model for remote estimation of chlorophyll-*a* in turbid waters: validation *Remote Sens. Environ.* **112** 3582–93

Gons H J 1999 Optical teledetection of chlorophyll-*a* in turbid inland waters *Environ. Sci. Technol.* **33** 1127–32

Gordon H R, Brown O B, Evans R H, Brown J W, Smith R C, Baker K S and Clark D K 1988 A semianalytic radiance model of ocean color *J. Geophys. Res.* **93** 10909–24

Gordon H R and Morel A Y 1983 Remote assessment of ocean color for interpretation of satellite visible imagery: a review *Lecture Notes on Coastal and Estuarine Studies* vol 4 (New York: Springer) p 114

Gordon H R and Wang M H 1994 Retrieval of water-leaving radiance and aerosol optical-thickness over the oceans with SeaWiFS—a preliminary algorithm *Appl. Opt.* **33** 443–52

Gower J F R, Doerffer R and Borstad G A 1999 Interpretation of the 685 nm peak in water-leaving radiance spectra in terms of fluorescence, absorption and scattering, and its observation by MERIS *Int. J. Remote Sens.* **20** 1771–86

Hu C M, Carder K L and Muller-Karger F E 2000 Atmospheric correction of SeaWiFS imagery over turbid coastal waters: a practical method *Remote Sens. Environ.* **74** 195–206

Moore G F, Aiken J and Lavender S J 1999 The atmospheric correction of water colour and the quantitative retrieval of suspended particulate matter in case II waters: application to MERIS *Int. J. Remote Sens.* **20** 1713–33

Morel A and Prieur L 1977 Analysis of variations in ocean color *Limnol. Oceanogr.* **22** 709–22

Moses W, Gitelson A, Berdnikov S and Povazhnyy V 2009 Satellite estimation of chlorophyll-*a* concentration using the red and NIR bands of MERIS—the Azov Sea case study *IEEE Geosci. Remote Sens. Lett.* at press doi:10.1109/LGRS.2009.2026657

O'Reilly J E *et al* 2000 *SeaWiFS Postlaunch Calibration and Validation Analyses* (*Part 3. NASA Tech. Memo. 2000-206892*) vol 11 (MD: NASA Goddard Space Flight Center) p 49

Ruddick K G, Ovidio F and Rijkeboer M 2000 Atmospheric correction of SeaWiFS imagery for turbid coastal and inland waters *Appl. Opt.* **39** 897–912

Wang M H and Shi W 2005 Estimation of ocean contribution at the MODIS near-infrared wavelengths along the east coast of the US: two case studies *Geophys. Res. Lett.* **32** L13606